Available online at www.sciencedirect.com
ScienceDirect
Carbohydrate Polymers 67 (2007) 623–629
Carbohydrate Polymers
www.elsevier.com/locate/carbpol

Depositing Cu_2O of different morphology on chitosan nanoparticles by an electrochemical method

Jin-Yi Chen [a,b], Pei-Jiang Zhou [a,*], Jia-Lin Li [b], Su-Qin Li [b]

[a] College of Resources and Environmental Sciences of Wuhan University, Wuhan 430072, PR China
[b] Nanotechnology Research Institute of Central China Normal University, Wuhan 430079, PR China

Received 18 April 2006; received in revised form 30 June 2006; accepted 3 July 2006
Available online 1 September 2006

Abstract

The chitosan nanoparticles were prepared with the least chemical productions by adding sodium sulfate. The cuprous oxide (Cu_2O)/chitosan nanocomposites were prepared by electrochemical deposition of nanocrystalline Cu_2O on chitosan nanoparticles. With the change of the reaction conditions, it was found that Cu_2O nanoparticles could be leafage-like or big spherical particles coated on the surface of chitosan nanoparticles. The composition of the resulting Cu_2O/chitosan composites was confirmed by using SEM images, XRD pattern, and XPS spectrum. The chemical interaction between Cu_2O and chitosan nanoparticles was probed into by FTIR spectrum. The Cu_2O/chitosan nanocomposites make it possible of seeking materials that can degrade pollutants with minimal energy and the least reagent under biocompatible and environmentally friendly conditions.

Keywords: Deposition; Electrochemical method; Cuprous oxide; Chitosan nanocomposites

1. Introduction

Chitosan (CS), due to its hydrophilicity, chemical reactivity, moldability, mechanical properties, biocompatibility, and biodegradability, is an excellent material that can be used in many areas such as food science, biochemistry, pharmaceuticals, medicine, agriculture, and so on (Domard & Piron, 2000; Sahidi, Arachchi, & Jeon, 1999; Vincendon, 1997; Marisa, Beppu, & Santana, 2001). CS, like most biopolymers, presents the property of being an ion-exchanger through chelating. Chelating ion exchange, in contrast to simple ion exchange, uses the three-dimensional structure of molecules to remove ions of specific sizes (Muzzarelli, Ferrero, & Pizzoli, 1972). More importantly, it exhibits an excellent capability to remove Cu (II) ions from aqueous solution (Deans & Dixon, 1991; Steenkamp, Keizer, Neomagus, & Krieg, 2002).

Cuprous oxide (Cu_2O) is a p-type semiconductor with a direct band gap of 2.0 eV (Yu, Du, Yu, Zhuang, & Wong, 2004), which offers it important applications in hydrogen production, and superconductor, solar cell, and negative electrode materials (Bohannan, Shumsky, & Switzer, 1999; Bordiga et al., 2001; Hara et al., 2000; Poizot, Laruelle, Grugeon, Dupront, & Taracon, 2000). It also has a potential application in photocatalytic degradation of organic pollutants under visible light (Ramirez-Ortiz, Ogura, & Medina-Valtierr, 2001). Cu^+ deposited on zeolite has been used for the photocatalytic decomposition of NO^x into N_2 and O_2 (Anpo et al., 1998). Cu_2O-activated carbon catalyst can decompose methanol to H_2 and CO directly (Tsoncheva, Nickdov, Vankova, & Mehandjiev, 2003). However, Cu_2O has not been commonly used because of the light-generated charge carriers in micron sized Cu_2O grains cannot be efficiently transferred to the surface and are lost due to recombination, which results in low solar energy conversion efficiency and its stability with respect to anodic photocorrosion. Therefore, the preparation of nanocrystalline Cu_2O materials is a key factor to improve the performance of the utilization of solar energy. But Cu_2O particles can reunite easily in nano-size. On the other hand, the importance of removing copper element from water is a well-known issue

* Corresponding author. Tel.: +86 27 87152823.
E-mail address: zhoupj@whu.edu.cn (P.-J. Zhou).

0144-8617/$ - see front matter © 2007 Published by Elsevier Ltd.
doi:10.1016/j.carbpol.2006.07.003

because although copper is an essential micronutrient, and is vital for the body in small amounts, in large amounts of it (over 1.3 mg/l) (Beppu, Arruda, Vieira, & Santos, 2004), humans can present symptoms from temporary stomach and intestinal disorders to kidney or liver damage depending on the time of exposure. The concentration of copper ions is an important factor to hold back the application of nano-sized Cu_2O particles in decontamination of waste water as a semiconductor photocatalyst. Thus, selecting coating supports which can not only fix and disperse nano-sized Cu_2O particles, but also remove copper ions formed in the course of photocatalytic degradation of pollutants, is a crucial for the common use of Cu_2O in the process of the decontamination of waste water. Several materials have been studied as supports such as multiwall carbon nanotubes (Ying et al., 2005), active carbon (Chu, Lei, Hu, & Yue, 1998), glass substrate (Lu, Chen, & Lin, 2005), and fiberglass (Medina-Valtierra, Calixto, & Ruiz, 2004), polycarbonate membrane (Daltin, Anne-Lise, Addad, Ahmed, & Jean-Paul Chopart, 2005). But none of them have all the following properties: dispersing and fixing the nano-sized Cu_2O to prevent the recombination with each other, chelateding copper ions firmly and removing them from solution, a good sorbent to adsorb various pollutants, environmental and biologic compatibility, and cheap and abundant starting material.

In this study, we attempted to find composite materials which can degrade pollutants with the least energy demand and reagents used, producing a minimum of by-products at low cost under ecological and environmental friendly conditions. The depositions of Cu_2O on the surface of chitosan under different conditions in the electrochemical process have been investigated. By changing the conditions in the preparation process, it is found that the assembled morphology of Cu_2O nanoparticles on the surface of chitosan can be easily controlled.

2. Experiment

2.1. Preparation of CS nanoparticles

CS from shrimp shells was purchased from Yuhuan Ocean Biochemical Co. (Zhejiang, China), whose degree of deacetylate (DD) was 92%, and whose molecular weight (Mw) was 210 kDa.

The nano-sized CS was prepared by the method described below: 2 g CS was dissolved in 100 ml 2% (V/V) acetic acid solution under magnetic stirring. When the solution became clear, 100 mg cetyltrimethyl ammonium bromide (CTAB) was added to the solution. Then, 25 ml of 20% Na_2SO_4 was added slowly to the solution with continued stirring. When the opalescent suspension appeared, the opalescent suspension was filtered with paper filter to remove any polymer aggregation, and then, the nanoparticles were dried for 2 h at 333 K.

2.2. Preparation of Cu_2O/CS nanoparticles

The experiments were performed in an electrolytic cell designed by ourselves (Jialin Li et al., 2004) (Fig. 1). The cell was divided into anodic and cathodal bathes by an anion exchange membrane. The anodic electrolyte was the aqueous solution of 300 g L^{-1} sodium chloride and a piece of copper plate was used as the anode, while the cathodal electrolyte was the aqueous solution of sodium hydroxide (1 mol L^{-1}) and a piece of stainless steel net was used as the cathode.

For the preparation of Cu_2O/CS particles composite, nano-sized CS was added into the anodic bath at the beginning of the reaction, the temperature of the reaction was controlled at about 353 K. During the reaction, perpetual agitating was necessary. The color of the solution changed to orange and then to brick red. When the reaction finished,

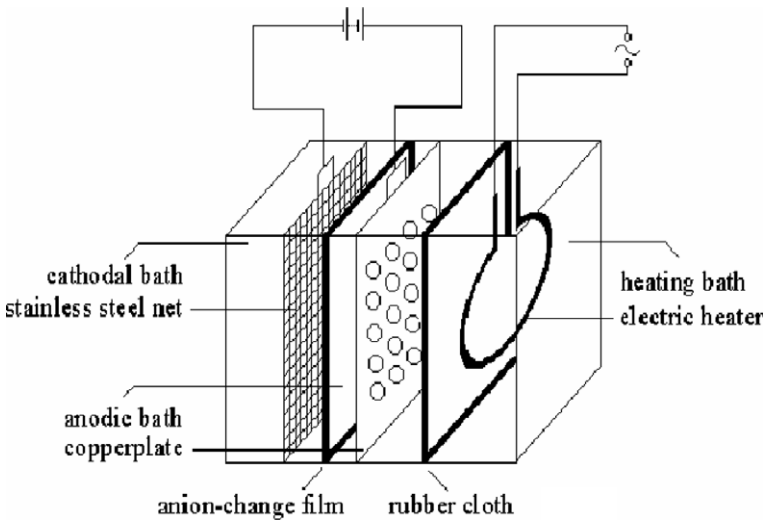

Fig. 1. The diagrammatic sketch of the electrolytic cell (a piece of 10×10 cm copper plate was used as the anode; a piece of stainless steel net with the same dimensions was used as the cathode).

the anodic electrolyte was taken out and centrifugated. Then, the deposition was washed immediately by distilled water till no chloride was in the deposition. In order to avoid Cu_2O being oxidized, the composite was immersed in the alcohol solution of 1‰ benzotriazole (BTA) for 2 h and then BTA in the composite was scoured off with ethanol. At last, the obtained composites were dried in vacuum at 333 K for 2 h.

The morphologies of the nanoconposites were performed by SEM. Their Fourier transform infrared spectroscopy (FTIR) was taken with KBr pellets on NEXUS™ FTIR (Thermo Nicolet Ltd. US). And their X-ray diffraction (XRD, Y-2000, Dandong) was taken on a X-ray powder diffractometer with CuK α radiation ($\lambda = 1.5418$ Å). X-ray photoelectron spectroscopy (XPS) measurements were performed by using a XSAM800 XPS system with Mg Ka radiation.

3. Results and discussion

3.1. SEM

The Fig. 2(a–d) shows a set of SEM images of Cu_2O/CS composite prepared under different conditions. Fig. 2(a) is the SEM image of nano-sized CS particles, which shows that the CS particles are about 100 nm in diameter and spherical in shape. When the electric current is at 0.05 A for 30 min, needle-shaped Cu_2O particles 20 nm in diameter and 50 nm in length deposited on CS nanoparticles (Fig. 2(b)). These needle-shaped Cu_2O are likely to grow directly on the surface of CS. When the electric current of the system keeps at 0.1 A for 30 min, the finally obtained composites are shown in Fig. 2(c), where no needle-shaped Cu_2O nanocrystalline but Cu_2O spherical nanoparticles are found on the surface of CS. When the electric current keeps at 0.6 A for more than 10 min, both needle-shaped nanocrystalline and big spherical particles of Cu_2O are found on the surface of CS (Fig. 2(d)). Therefore, the morphology of the Cu_2O crystal depositing on the CS could be easily controlled by the change of the experimental parameters.

The reason that different currents produce different morphologies of Cu_2O on the surfaces of CS particles may be described as follows (Zhang, Li, Chen, Tang, & Yu, 2006): Anodic reaction (anodic dissolution of copper):

$$Cu + nCl^- - e^- \rightarrow CuCl_n^{1-n} (n = 2, 3) \quad (1)$$

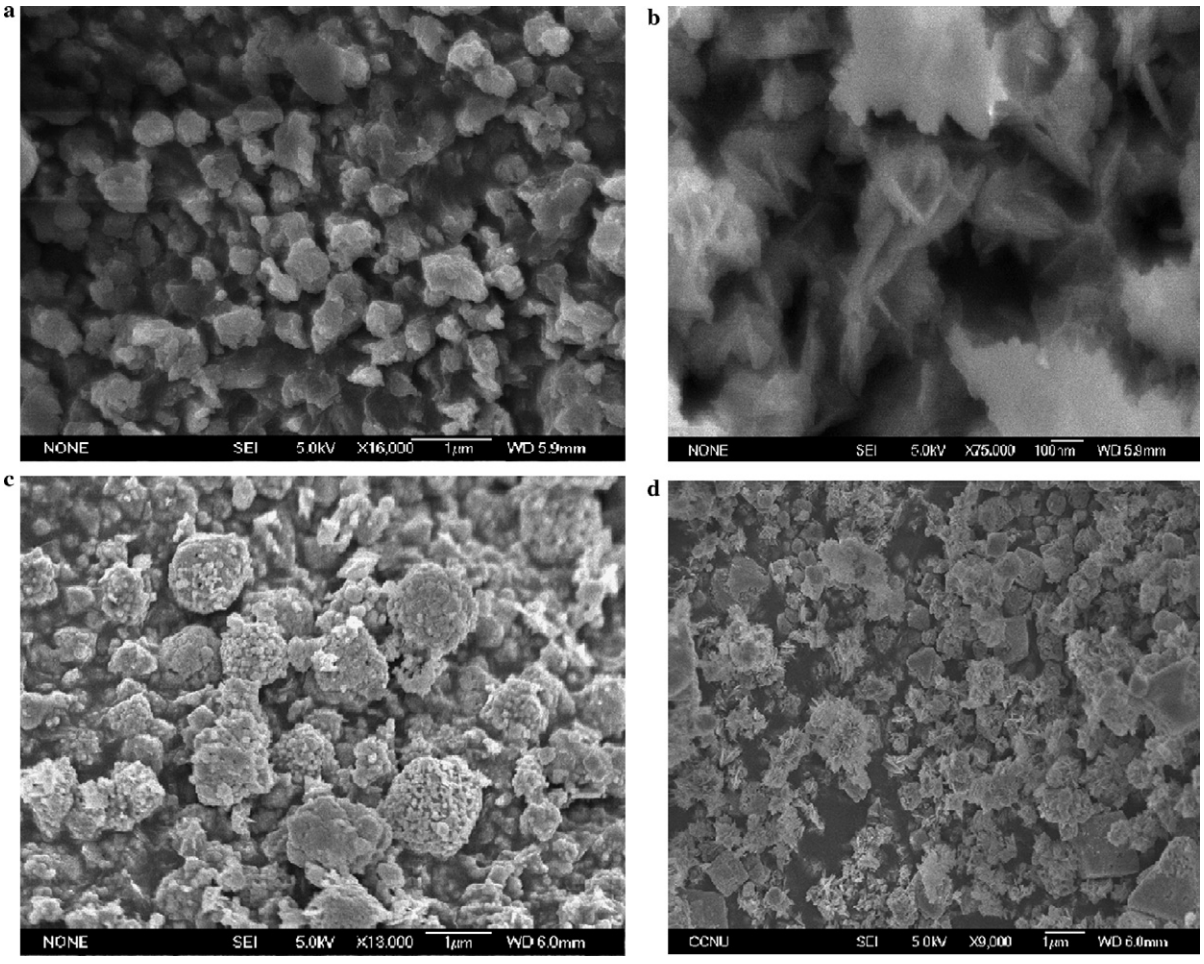

Fig. 2. The SEM images of CS and Cu_2O/CS composites. (a) Nano-CS particles; (b) Cu_2O/CS prepared under the current of 0.05 A for 30 min; (c) Cu_2O/CS prepared under the current of 0.1 A for 30 min; (d) Cu_2O/CS prepared under the current of 0.6 A for 10 min.

Cathodic reaction (hydrogen evolution):

$$2H_2O + 2e^- \rightarrow H_2 \uparrow + 2OH^- \quad (2)$$

Chemical reactions (hydrolysis precipitation):

$$CuCl_n^{1-n} + 2OH^- \rightarrow Cu(OH)_2^- + nCl^- \ (n = 2, 3) \quad (3)$$

$$2Cu(OH)_2^- \rightarrow Cu_2O \downarrow + H_2O + 2OH^- \quad (4)$$

Thus the net cell reaction is the summation of Eqs. (1)–(4), that is:

$$2Cu + H_2O = H_2 \uparrow + Cu_2O \quad (5)$$

Based on the above mechanism, we can draw a conclusion from equation (1) and (2) that the anode copper plate dissolve slowly when the current is set at 0.05 A. That the concentration of $CuCl_n^{1-n}$ and OH^- in the solution was low can keep the concentration of $Cu(OH)_2^-$ at a low level so as to make it react with the amino group on CS to form the CS–$NH_2^+ - Cu(OH)_2^-$ ion pair. The crystal nucleuses of Cu_2O grow slowly on CS along the ⟨1 1 1⟩ direction and a needle-shaped nanocrystalline is formed finally.

But when the current was increased to 0.1 A, the concentration of $CuCl_n^{1-n}$ and OH^- in the solution will become higher than that at 0.05 A, the other lattice planes will also grow slowly after the growth of dominance lattice plane ⟨1 1 1⟩ with the result that all the Cu_2O lattice planes were filled in to form the Cu_2O granular nanoparticles, which deposit around the CS nanoparticles finally.

When the current increased to 0.6 A, the anode copper plate dissolved faster than that at low current according to Eqs. (1) and (2). So, the concentration of $CuCl_n^{1-n}$ and OH^- in the solution rapidly increased accordingly. It is indicated that the hydrolysis of $CuCl_n^{1-n}$ should be accelerated to and generate more $Cu(OH)_2^-$ in a short time so that it cannot be dispersed by CS in time. Therefore, some $Cu(OH)_2^-$ can also react with the amino group on CS nanoparticles and form the Cu_2O needle-shaped nanocrystalline. Others that have not reacted with CS can grow and aggregate together to form the spherical particles of Cu_2O on CS. The different morphologies of Cu_2O can coexist because the morphologies of Cu_2O/CS nanocomposites in Fig. 2(c) were obtained in short time.

3.2. XRD

The typical powder X-ray diffraction (XRD) patterns of the nano-sized CS, Cu_2O and Cu_2O/CS composites were shown in Fig. 3. The XRD pattern of nano-sized CS (Fig. 3(a)) shows the characteristic crystalline peaks at around $2\theta = 15.16°$, $2\theta = 22.84°$. And in the XRD pattern of nano-sized Cu_2O (Fig. 3(c)), all the peaks are clearly distinguished. There are five peaks with 2θ values of 29.84, 36.72, 42.6, 61.72, and 74.04, corresponding to (1 1 0), (1 1 1), (2 0 0), (2 2 0) and (3 1 1) crystal planes of pure Cu_2O, respectively. And the peak at $2\theta = 15.16°$ and 22.84 corresponds to the CS. Meanwhile, the (1 1 1) reflection of the samples obtained is relatively strong. Interplanar distances calculated for (1 1 0), (1 1 1), (2 0 0), (2 2 0),

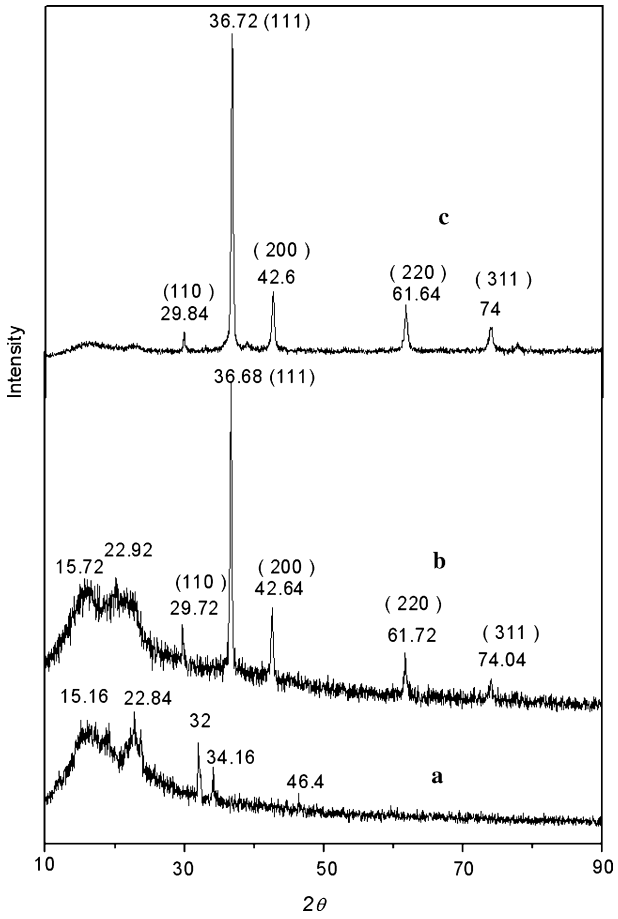

Fig. 3. The XRD patterns of CS, Cu_2O and Cu_2O/CS nanocomposites. (a) Nano-CS particles; (b) Cu_2O/CS nanocomposites prepared under the current of 0.05 A for 30 min; (c) pure Cu_2O nanocrystalline prepared under the current of 0.05 A for 30 min.

and (3 1 1) from XRD patterns match well with standard data confirming the formation of Cu_2O. No other diffraction peaks arising from metal Cu or CuO appear in the XRD patterns. After incorporating Cu_2O with CS, the basal planes diffraction peaks of CS at $2\theta = 22.84°$, $2\theta = 32°$ and $2\theta = 34.16°$ disappear (Fig. 3(b)), substituted by a new broad peak at around $2\theta = 20$–$22.92°$. The absence of these peaks in the XRD with Cu_2O indicates that complexation has occurred between the Cu_2O and the CS. The variation of the basal diffraction of CS indicates the formation of an interaction with Cu_2O. However, it is difficult for XRD to give definitive conclusions about the defined structure. Thus, FTIR techniques are necessary to characterize the morphology of the Cu_2O/CS nanocomposites.

3.3. FTIR spectra

The FTIR spectra of CS, Cu_2O and Cu_2O/CS nanoparticles were shown in Fig. 4. Fig. 4(a) depict characteristic absorption bands at 3441 and 2879 cm^{-1}, which represent the –NH_2, –OH, and –CH_2, –CH_3 aliphatic groups, and bands at 1597 and 1422 cm^{-1} which represent the amino group bending vibration and vibrations of –OH group of

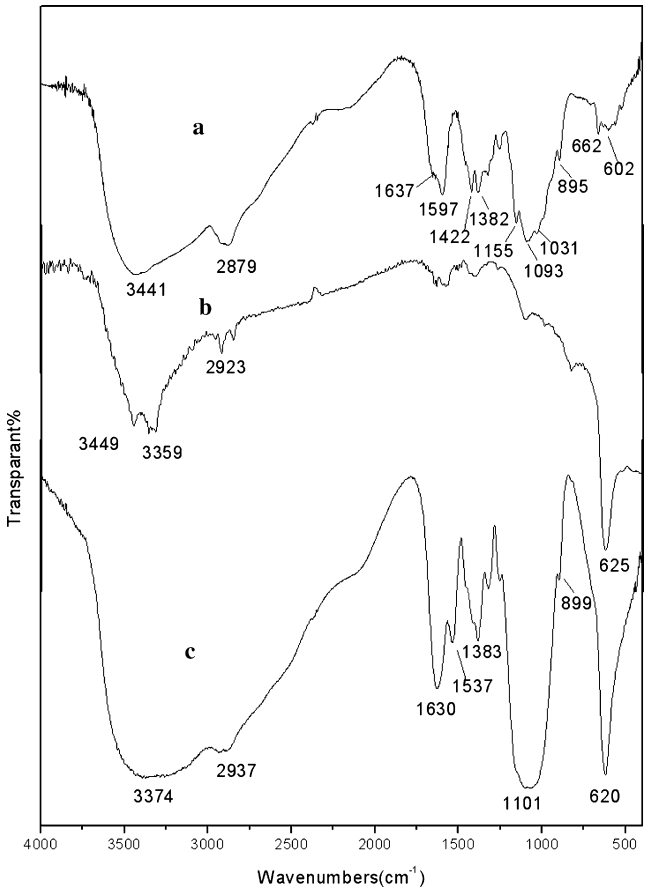

Fig. 4. The FTIR spectra of CS, Cu_2O and Cu_2O/CS nanocomposites. (a) Nano-CS particles; (b) pure Cu_2O nanocrystalline prepared under the current of 0.05 A for 30 min; (c) Cu_2O/CS nanocomposites prepared under the current of 0.05 A for 30 min.

the primary alcoholic group, respectively. The amino group has a characteristic absorption band in the region of $3400 \sim 3500\ cm^{-1}$, which is masked by the broad absorption band from the –OH group. The shoulder at $1637\ cm^{-1}$ represents the C═O groups and suggests CS is a partially deacetylated product (90%). The spectra of Cu_2O nanoparticles (Fig. 4(b)) show the characteristic absorption bands at $625\ cm^{-1}$ (Dambies, Guimon, Yiacoumi, & Guibal, 2001; Ngah, Endud, & Mayanar, 2002), and bands at 3449 and $3359\ cm^{-1}$, which represent the –OH groups (from water molecule absorbed on the surface of Cu_2O nanoparticles). When CS combined with Cu_2O, more pronounced shift in the FTIR spectrum could be observed in the complexes (Fig. 4(c)).The major differences are: the wide peak at $3441\ cm^{-1}$, corresponding to the stretching vibration of amino group and hydroxy group, shifted to lower frequency ($3374\ cm^{-1}$), and the peak of $3374\ cm^{-1}$ becomes wider, which indicates hydrogen bonding is enhanced and may be explained as that the additive effect of water absorbed on the surface of Cu_2O nanoparticles (3449 and $3359\ cm^{-1}$ in Fig. 4(b)) and the –OH group of CS. Additionally, the wide absorb peak at 3441 and $1597\ cm^{-1}$ in Fig. 4(a), which represent the stretching vibration and the bending vibration of amino group, disappeared and a new absorb peak at $1630\ cm^{-1}$ appeared, which indicated that the amino group was involved in complexation. Meanwhile, the characteristic peak of Cu_2O in Fig. 4(c) also has five changes of wavenumbers change compared with characteristic absorption bands in Fig. 4(b), from 625 to $620\ cm^{-1}$. This significant shift of the characteristic peaks and increase of the intensity result from the strong interaction between CS and Cu_2O.

Fig. 5 represents the FTIR spectra of pure CS and Cu_2O/CS nanoparticles with increasing ratio of Cu_2O (up to 2:1) and different methods for combination. The pure CS (Fig. 5(a)) showed absorption bands at 1637 and $1093\ cm^{-1}$, attributing to the amide carbonyl and C–O stretching, respectively. Fig. 5(b) represents the spectra of pure CS physical mixed up (PM) with Cu_2O nanoparticles at the ratio of 1:1. There is hardly any noticeable shift in peaks of the CS as presented in this figure. Hence, the Cu_2O/CS (PM) system is a mixed phase with no interaction with one another. Contrasting with CS and Cu_2O/CS

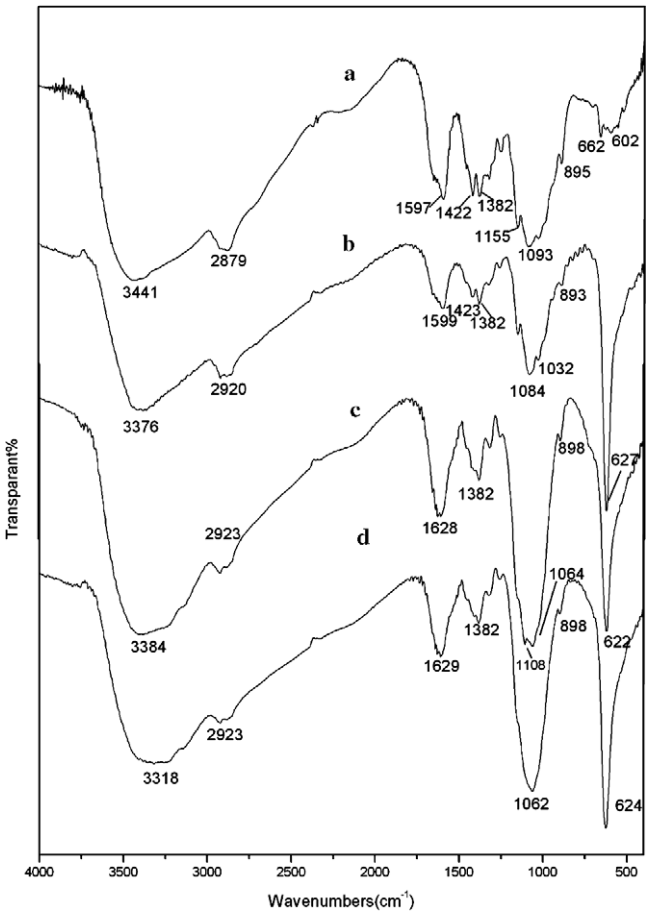

Fig. 5. The FTIR spectra of pure CS and Cu_2O/CS nanoparticles with increasing ratio of Cu_2O (up to 2:1) and different methods for combination. (a) Pure CS; (b) pure CS physical mix up (PM) with Cu_2O nanoparticles at the mass ratio of 1:1; (c) Cu_2O/CS nanocomposites at the mass ratio of 1:1 by electrodeposition; (d) Cu_2O/CS nanocomposites at the mass ratio of 2:1 by electrodeposition.

(PM), there are several noticeable shifts in peaks of the Cu_2O/CS nanoparticles as presented in this figure.

These features that have been described above (Fig. 4) are also observed in the spectra of these samples containing different ratio of Cu_2O. At low Cu_2O ratio (1:1) (Fig. 5(c)), the wide peak of the stretching vibration of $-NH_2$ group and –OH group at 3441 cm^{-1} shifted to lower frequency (3384 cm^{-1}), and the peak of 3384 cm^{-1} becomes wider. Additionally, the absorb peak at 1597 and 1422 cm^{-1} in Fig. 5(a) disappeared and a new absorb peak at 1628 cm^{-1} appeared. As the Cu_2O ratio reaches 2:1 (Fig. 5(d)) the wide peak of the stretching vibration of $-NH_2$ group and –OH group at 3384 cm^{-1} shifted to lower frequency (3318 cm^{-1}), and the peak of 3318 cm^{-1} becomes wider again. So, the frequency of the stretching vibration of $-NH_2$ and –OH group became lower with the increasing Cu_2O ratio, which shows the interaction between CS and Cu_2O nanoparticles enhanced with the Cu_2O ratio increased. The characteristic peaks of the binding vibration of amide (II) at 1597 cm^{-1} that appeared in the spectra of the CS and the Cu_2O/CS (PM) nearly disappeared in the spectra of Cu_2O/CS nano-sized composites. The C–O stretching vibrations of the Cu_2O/CS after electrochemical deposition shifted to lower wave number (1062 cm^{-1}). To sum up, the FTIR results indicated that the interaction between CS and Cu_2O in Cu_2O/CS nano-sized composites prepared by electrochemical deposition is much stronger than that in the Cu_2O/CS system prepared by physical mix up.

3.4. XPS

The XPS analysis was carried out with a spectrometer (XSAM800, model M-probe, Kratos Ltd. (UK)). Fig. 6 shows the high resolution XPS spectrum for the Cu2p core level for the Cu_2O/CS composite. The peak at 932.5 eV, corresponding to the binding energy of $Cu2p_{3/2}$, is in good agreement with data observed for copper (I) oxide (Nikesh, Mandale, Patil, & Mahamuni, 2005). It shows that the resultant nanoparticles were Cu_2O and the binding process did not result in the phase change of Cu_2O.

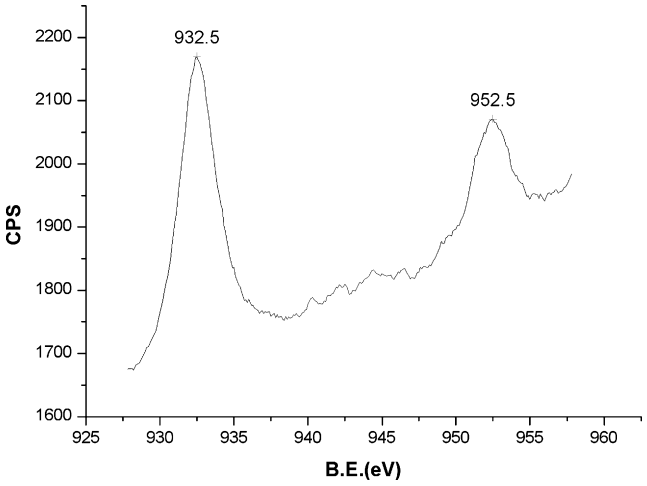

Fig. 6. The high resolution XPS spectrum for the Cu2p core level for the Cu_2O/CS composite.

4. Conclusions

Cu_2O/CS chitosan composites were prepared by the electrochemical method. This method arises from an industrial procedure with minor modification, so it is simple, reliable, and easy to carry out on a large scale. The analyses of SEM, XRD, FTIR, and XPS indicated that the CS interacted with Cu_2O nanoparticles through the $-NH_2$ and the –OH groups in the CS, which did not change the structure of Cu_2O.

Acknowledgment

The work is financially supported by National Natural Science Foundation of China (No. 20207002).

References

Anpo, M., Matsuoka, M., Hanou, K., Mishima, H., Yamashita, H., & Patterson, H. H. (1998). The relationship between the local structure of copper(I) ions on Cu^+/zeolite catalysts and their photocatalytic reactivities for the decomposition of NO_x into N_2 and O_2 at 275 K. *Coordination Chemical Reviews, 171*(1), 175–184.

Beppu, M. M., Arruda, E. J., Vieira, R. S., & Santos, N. N. (2004). Adsorption of Cu (II) on porous CS membranes, functionalized with histidine. *Journal of Membrane Science, 240*, 227–235.

Bohannan, E. W., Shumsky, M. G., & Switzer, J. A. (1999). Epitaxial electrodeposition of copper (I) oxide on single-crystal gold (100). *Chemical Materials, 11*(9), 2289–2291.

Bordiga, S., Paze, C., Berlier, G., Scarano, D., Spoto, G., Zechina, A., et al. (2001). Interaction of N_2, CO and NO with Cu-exchanged ETS-10: a compared FTIR study with other Cu–zeolites and with dispersed Cu_2O. *Catalysis Today, 70*, 91–105.

Chu, H. P., Lei, L., Hu, X., & Yue, P. L. (1998). Metallo-organic chemical vapor deposition (MOCVD) for the development of heterogeneous catalysts. *Energy and Fuels, 12*(6), 1108–1113.

Daltin Anne-Lise Addad Ahmed & Jean-Paul Chopart (2005). Potentiostatic deposition and characterization of cuprous oxide films and nanowires. *Journal of Crystal Growth, 282*, 414–420.

Dambies, Laurent, Guimon, Claude, Yiacoumi, Sotira, & Guibal, Eric (2001). Characterization of metal ion interactions with CS by X-ray photoelectron spectroscopy. *Colloids and Surfaces A: Physicochemical and Engineering Aspects, 177*, 203–214.

Deans, J. R., & Dixon, B. G. (1991). Uptake of Pb^{2+} and Cu^{2+} by novel biopolymers. *Water Research, 26*, 469.

Domard, A., & Piron, E. (2000) Recent approach of metal binding by CS and derivatives. In: M. G. Peter, A. Domard, R. A. A. Muzzarelli (Eds.), *Advances in Chitin Science, 4*, pp. 295–301.

Hara, M., Hasei, H., Yashima, M., Ikeda, S., Takata, T., Kondo, J., et al. (2000). Mechano-catalytic overall water splitting (II) nafion-deposited Cu_2O. *Applied Catalysis A: General, 190*(1–2), 35–42.

Li, Jialin, Liu, Li, Yu, Ying, Tang, Yiwen, Li, Huanlun, & Du, Feipeng (2004). Preparation of highly photocatalytic active nano-size TiO_2–Cu_2O particle composites with a novel electrochemical method. *Electrochemistry Communications, 6*, 940–943.

Lu, Yang-Ming, Chen, Chun-Yuan, & Lin, Ming Hong (2005). Effect of hydrogen plasma treatment on the electrical properties of sputtered N-doped cuprous oxide films. *Thin Solid Films, 480–481*, 482–485.

Medina-Valtierra, Jorge, Calixto, Sergio, & Ruiz, Facundo (2004). Formation of copper oxide films on fiberglass by adsorption and reaction of cuprous ions. *Thin Solid Films, 460*, 58–61.

Marisa, M., Beppu, M. M., & Santana, C. C. (2001). In vitro biomineralization of chitosan. *Key Engineering Materials, 31*, 192–195.

Muzzarelli, R. A. A., Ferrero, A., & Pizzoli, M. (1972). Light-scattering X-ray diffraction, elemental analysis and infrared spectrophotometry characterization of CS, a chelating polymer. *Talanta, 19*, 1222–1226.

Ngah, W. S., Endud, W. C. S., & Mayanar, R. (2002). Removal of copper (II) ions from aqueous onto CS and cross-linked CSs beads. *Reactive and Functional Polymers, 50*, 181.

Nikesh, V. V., Mandale, A. B., Patil, K. R., & Mahamuni, S. (2005). X-ray photoelectron spectroscopic investigations of Cu_2O nanoparticles. *Materials Research Bulletin, 40*, 694–700.

Poizot, P., Laruelle, S., Grugeon, S., Dupront, L., & Taracon, J. M. . *Nature, 407*, 496.

Ramirez-Ortiz, J., Ogura, T., & Medina-Valtierr, J. A. (2001). A catalytic application of Cu_2O and CuO films deposited over fiberglass. *Applied Surface Science, 174*(3–4), 177.

Sahidi, F., Arachchi, J. K. V., & Jeon, Y. J. (1999). Food applications of chitin and CSs: review. *Trends Food Science and Technology, 10*, 37.

Steenkamp, G. C., Keizer, K., Neomagus, H. W. J. P., & Krieg, H. M. (2002). Copper (II) removal from polluted water with alumina/CS composite membrane. *Journal of Membrane Science, 197*, 147.

Tsoncheva, T., Nickdov, R., Vankova, S., & Mehandjiev, D. (2003). *Canadian Journal of Chemistry, 81*, 1096.

Vincendon, M. (1997). Regenerated chitin from phosphoric acids solutions. *Carbohydrate Polymers, 32*, 233.

Yu, Ying, Ma, Li-Li, Huang, Wen-Ya, Li, Jia-Lin, Wong, Po-Keung, & Yu, Jimmy C. (2005). Coating MWNTs with Cu_2O of different morphology by a polyol process. *Journal of Solid State Chemistry, 178*, 1488–1494.

Yu, Y., Du, F. P., Yu, J. C., Zhuang, Y. Y., & Wong, P. K. (2004). *Journal of the Solid State Chemistry, 177*, 4640.

Zhang, Lisha, Li, Jialin, Chen, Zhigang, Tang, Yiwen, & Yu, Ying (2006). Preparation of Fenton regent with H_2O_2 generated by solar light-illuminated nano-Cu_2O/MNTs composites. *Applied Catalysis A: General, 299*, 22–97.